

ARTICLE TYPE

Fixed-time synchronization of coupled memristive neural networks with multi-links and application in secure communication [†]

Hui Zhao*¹ | Aidi Liu¹ | Qingjie Wang¹ | Mingwen Zheng² | Chuan Chen³ | Sijie Niu*¹ | Baozhu Li¹

¹Shandong Provincial Key Laboratory of Network Based Intelligent Computing, School of Information Science and Engineering, University of Jinan, Jinan 250022, China

²School of Mathematics and Statistics, Shandong University of Technology, Zibo 255000, China

³School of Cyber Security, Qilu University of Technology (Shandong Academy of Sciences), Jinan 250353, China

Correspondence

*Hui Zhao, Sijie Niu.

Email: hz_paper@163.com(Hui Zhao), sjniu@hotmail.com(Sijie Niu)

Present Address

This is sample for present address text
this is sample for present address text

Summary

This paper is devoted to investigating the issues of fixed-time synchronization of coupled memristive neural networks with multi-links (MCMNN). Based on the fixed-time stability criterion and the upper bound estimate formula for the settling time, we propose a secure communication scheme. The network with multi-links performance and coupled form increase the complexity of network topology and the unstable of systems, which improve security of communication in the aspect of encrypt the plaintext signal. We design a proper controller and build the Lyapunov function, several effective conditions are obtained to achieve the fixed-time synchronization of MCMNN. Moreover, the settling times can be estimated for fixed-time synchronization without depending on any initial values. Meanwhile, the plaintext signals can be recovered according to the fixed-time stability theorem. Finally, numerical simulations are given to verify the effectiveness of the theoretical results in fixed-time synchronization of MCMNN, and an example of a secure communication scheme is given to show the usability and superiority based on fixed-time stability theorem.

KEYWORDS:

Fixed-time synchronization, coupled memristive neural network, multi-links topology, secure communication scheme

1 | INTRODUCTION

As the development of information technology, the requirement of information transmission quantity and quality is higher and higher. The security of communication becomes very important, secure communication has been focused on by researchers. Meanwhile, the synchronization of chaotic systems have been applied to secure communication at home and abroad^{1,2,3,4}. The main considered problems include secure transmission performance in synchronization time and the encryption performance based on chaotic system.

The types of synchronization time include asymptotic time synchronization, exponential synchronization and finite-time synchronization. Many previous studies have made important contributions to the convergence of synchronization

[†]This is an example for title footnote.

time^{5,6,8}. The asymptotic time synchronization and exponential synchronization are infinite time synchronization, but the convergence rate of exponential time is slightly faster than that of asymptotic time. However, the finite-time stability has more practical significance in secure communication. The finite time was introduced in 1961⁹, which has much faster convergence time. In the secure communication, compared with asymptotic synchronization and exponential synchronization, the finite-time synchronization technique enables us to recover the transmitted signals in a setting time, which improves the efficiency and the confidentiality greatly. The concept of fixed time stability is proposed of Polyakov in 2012¹⁰, and the criteria for determining whether the system can achieve fixed time stability are also gave. Fixed time stability is a special kind of finite time stability. It is different from general finite time stability in that its stability time has a definite upper bound, which does not depend on the initial value of the system, but only related to the system parameters and controller parameters. Therefore, the insensitivity of fixed time stability to initial value and the controllability of stable time are still a hot research field.

The types of chaotic systems include simple three-dimension chaotic systems, complex dynamical networks and general neural networks etc.. Like neural network, memristive neural network is also a kind of chaotic system, but is different from neural network on that the parameters of MNN are state-dependent. Memristor was first proposed by Leon Chua in 1971¹¹, Unlike ordinary resistors, which have fixed resistance values, the memristor is nonlinear one and its value is not unique, the memristor was also considered to be the electronic equivalent of the synapse. As the memristor is well used to mimic the synapse, the model of MNN is widely applied in the associative memory, the next generation computer and powerful brain-like "neural" computer, MNN is the more realistic model for the description of real neural systems. Therefore, there has been an upsurge in the study of dynamic behavior based on the model of MNN.

Recently, researches on synthesis of the fixed time stability theory and memristive neural network model are in full swing. The related applications have also been proposed^{12,13}. In 2017, Cao etc. studied the fixed time synchronization of memristive recurrent neural networks based on feedback control for the first time¹⁴, and gave the corresponding fixed time synchronization criteria. The upper bound estimation of synchronization time can also be changed by adjusting the control gain. The fixed-time synchronization of the memristor-based bidirectional associative memory neural network, the memristor-based fuzzy cellular neural network and the memristor-based Cohen-Grossberg neural networks are investigated respectively based on the proper controller and impulsive effects^{8,15,16}. Reference¹⁷ gave a new fixed-time stability theorem and applies to the fixed-time synchronization control of memristive neural networks. Reference^{18,19} studied the fixed time synchronization of inertial memristive neural networks with time-varying delays and with discrete time delay respectively. Meanwhile, the paper about the delayed memristor-based recurrent neural networks, the impulsive memristor-based neural networks, the stochastic memristor-based neural networks with adaptive control and the quaternion-valued memristive neural networks are studied to achieve the fixed-time synchronization^{20,21,22,23}. Furthermore, some papers considered the coupled topology, investigated the fixed-time synchronization of the coupled memristor-based neural networks with or without any time-delays^{24,25,26}. But, few papers take full of the coupled topology and multi-links performance to explore the fixed-time stability of the systems. Some application on image encryption and decryption scheme in Reference²⁷ and secure communication scheme in Reference¹² based on the fixed-time stability are given to show the usability and superiority of the obtained theoretical result. But, few papers gave the application on the fixed-time synchronization of coupled memristive neural network with multi-links. The detail contents of the multi-links performance about complex networks can refer to References^{13,28}.

Motivated by the above discussions, the multi-links performance, coupled forms and synchronization time of systems are taken fully into account in this paper. We investigate the fixed-time synchronization of MCMNN and design an efficient secure communication scheme based on fixed-time stability. The contribution of this paper are given as follows: Firstly, we overcome these complexity of the factors interaction include the multi-links performance and coupled forms, dealing with some parameter mismatches and complex topological structure problems, the MCMNN studied in this paper is more complex and general than others neural networks. Therefore, the network model are more general; Secondly, the fixed-time synchronization issue of drive-response MCMNN is first studied based on the feedback controller and give a new fixed-time stable theorem. The fixed-time stability is more useful than exponent and finite-time stability in application; Thirdly, the secure communication scheme is designed based on fixed-time synchronization of drive-response MCMNN. The upper time of the fixed time can be as an important common key,

the plaintext signal can be recovered after the upper time. Finally, numerical simulation and the example of secure communication are given to verify the effectiveness of our theoretical results.

The paper is organized as follows. In Section 2, the model of MCMNN and preliminaries are given. In Sections 3, The fixed-time synchronization theorem and corollaries are respectively given. In Section 3, we designed the security communication scheme based on fixed-time synchronization of MCMNN. The numerical example of the fixed-time stable and application example of secure communication scheme are given to show the effectiveness of our theoretical results in Section 5. Finally, concluding remarks are given in Section 6.

2 | NETWORK MODEL AND PRELIMINARIES

In the paper, according to the property of multi-links coupled topology, we consider a model of MCMNN as follows:

$$\begin{aligned} \dot{x}_{ik}(t) = & -c_k x_{ik}(t) + \sum_{q=1}^n a_{kq}(x_{ik}(t)) \bar{g}_q(x_{ik}(t)) \\ & + \sum_{q=1}^n b_{kq}(x_{ik}(t - \tau_0)) g_q(x_{ik}(t - \tau_0)) \\ & + \sigma \sum_{j=1}^N w_{ij}^0 \Gamma x_{jk}(t) \\ & + \sigma \sum_{l=1}^m \sum_{j=1}^N w_{ij}^l \Gamma x_{jk}(t - \tau_l) + I_i(t), \end{aligned} \quad (1)$$

where $x_i = (x_{i1}, x_{i2}, \dots, x_{in})^T \in R^n, i = 1, 2, \dots, N$ is the state vector of the i th node; $C = \text{diag}(c_1, c_2, \dots, c_n)$ is a positive matrix and denotes the decay rates to the i th neuron; $\bar{g}(x_i(t)) = (\bar{g}_1(x_{i1}(t)), \bar{g}_2(x_{i2}(t)), \dots, \bar{g}_n(x_{in}(t))) \in R^n$ and $g(x_i(t - \tau_0)) = (g_1(x_{i1}(t - \tau_0)), g_2(x_{i2}(t - \tau_0)), \dots, g_n(x_{in}(t - \tau_0))) \in R^n$ are the discontinuous feedback function, τ_0 is time delay; σ represents the coupling strength; $\Gamma = \text{diag}(\gamma_1, \gamma_2, \dots, \gamma_n) > 0$ is the inner coupling matrix between each pair of nodes; $W_0 = (w_{ij}^0)_{N \times N}, W_l = (w_{ij}^l)_{N \times N}, l = 1, \dots, m$ represents the outer coupling configuration matrix of MNN, which is the different sub-network's Laplacian matrix, $\tau_l (l = 1, \dots, m) > 0$ denote different time-delays in the sub-networks. If node i and j are linked by an edge, then $w_{ij}^l = w_{ji}^l > 0 (i \neq j)$; otherwise, $w_{ij}^l = w_{ji}^l = 0$, and the diagonal elements of matrix W_l are defined as $w_{ii}^l = -\sum_{j=1, j \neq i}^N w_{ij}^l$. If there are no isolated nodes in the network, then all of the matrix $W_l (l = 0, 1, \dots, m)$ is an irreducible real symmetric matrix. $I(t) = (I_1(t), I_2(t), \dots, I_N(t))^T \in R^n$ is the external input.

The parameters $a_{kq}(x_{ik}(t))$ and $b_{kq}(x_{ik}(t - \tau_0))$ denote the non-delayed and delayed memristor-based synaptic connection weights, respectively. They can be described as follows:

$$a_{kq}(x_{ik}(t)) = \begin{cases} \hat{a}_{kq}, & |x_{ik}(t)| \leq T_i, \\ \check{a}_{kq}, & |x_{ik}(t)| > T_i, \end{cases} \quad (2)$$

$$b_{kq}(x_{ik}(t - \tau_0)) = \begin{cases} \hat{b}_{kq}, & |x_{ik}(t - \tau_0)| \leq T_i, \\ \check{b}_{kq}, & |x_{ik}(t - \tau_0)| > T_i, \end{cases} \quad (3)$$

where the switching jumps $T_i > 0, \hat{a}_{kq}, \check{a}_{kq}, \hat{b}_{kq}, \check{b}_{kq}, k, q = 1, 2, \dots, n$, are all constants.

Remark 1. Generally speaking, digital computer applications only need two memory states, memristor only needs to show two sufficiently significant equilibrium states. Therefore, we assume that the memristor switches only between two states according to the voltage current characteristics. The pinched hysteresis loop is due to the nonlinear relationship between the memristance current and voltage which is shown in Figure 1(b), the simplified state curve is shown in Figure 1(a).

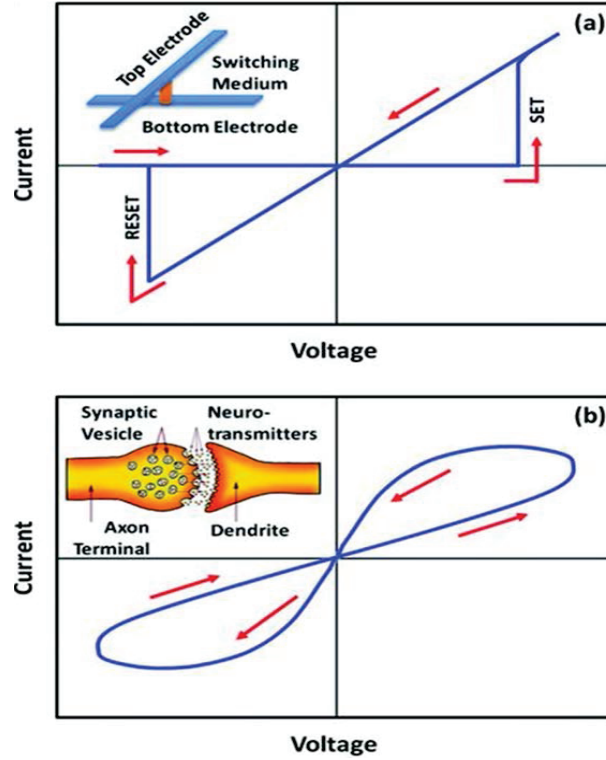


FIGURE 1 Typical current-voltage (i-v) characteristics of a memristor.

If the Eq.(1) is called as drive system, the corresponding response system with a control input can be characterized by:

$$\begin{aligned}
 \dot{y}_{ik}(t) = & -c_k y_{ik}(t) + \sum_{q=1}^n a_{kq}(y_{ik}(t)) \bar{g}_q(y_{ik}(t)) \\
 & + \sum_{q=1}^n b_{kq}(y_{ik}(t - \tau_0)) g_q(y_{ik}(t - \tau_0)) \\
 & + \sigma \sum_{j=1}^N w_{ij}^0 \Gamma y_{jk}(t) \\
 & + \sigma \sum_{l=1}^m \sum_{j=1}^N w_{ij}^l \Gamma y_{jk}(t - \tau_l) + I_i(t) + u_{ik}(t),
 \end{aligned} \tag{4}$$

where $i, j = 1, 2, \dots, N$, $y_i = (y_{i1}, y_{i2}, \dots, y_{in})^T \in R^n$ is the state vector of the i th node of the response network and $u_{ik}(t)$ is the controller for node i . The remainder parameters of Eq.(4) have the same meanings as those in Eq.(1).

Definition 1. (Filippov Regularization²⁹) For differential system, $\dot{x}(t) = f(t, x)$, where $f(t, x)$ is discontinuous in $x(t)$ and $x(t)$ is a solution of the differential system on $[t_0, t_1]$ in Filippov's sense, if $x(t)$ is absolutely continuous on any compact interval $[t_0, t_1]$, for almost all $t \in [t_0, t_1]$ such that

$$\dot{x} = K_F[f](t, x)$$

where

$$K_F[f](t, x) = \bigcap_{\delta > 0} \bigcap_{\mu(N)=0} \overline{\text{co}}[f(B(x, \delta) \setminus N), t]$$

where $\overline{\text{co}}[\cdot]$ is the convex closure hull of a set, $B(x, \delta) = \{y : \|y - x\| \leq \delta\}$ is the ball of center x and radius δ , intersection is taken over all sets N of measure zero and over all $\delta > 0$, and $\mu(N)$ is Lebesgue measure of set N .

Definition 2. The drive-response system (1) and (4) are said to achieve the fixed-time synchronization if there exists $T(e_0(t))$ in some finite time such that

$$\begin{cases} \lim_{t \rightarrow T(e_0(t))} \|e(t)\| = 0, \\ e(t) = 0, \forall t \geq T(e_0(t)), \\ T(e_0(t)) \leq T_{\max}, \forall e_0(t) \in C^m[-\tau, 0]. \end{cases}$$

where T_{\max} is the settling time, $\|\cdot\|$ represents the Euclidean norm.

Assumption 1. For the neuron activation functions $\bar{g}_q(\cdot), g_q(\cdot)$, there exists Lipschitz constants \bar{g}_q and $g_q > 0$ satisfying the following Lipschitz conditions:

$$\|\bar{g}_q(y) - \bar{g}_q(x)\| \leq \bar{f}_q \|y - x\|,$$

$$\|g_q(y) - g_q(x)\| \leq f_q \|y - x\|, x, y \in R.$$

Assumption 2. There exists a real number M_l such that $f_l(x) \leq M_l$, for all $x \in R, l = 1, 2, \dots, n$.

Lemma 1. (see³⁰) If there exists a regular, positive definite and radially unbounded function $V(e(t)) : R \rightarrow R$ and constants $a, b, \eta, k > 0$ and $\eta k > 1$ meet

$$\dot{V}(e(t)) \leq -(aV^\eta(t) + b)^k, t \in R^n \setminus 0,$$

then the origin is fixed-time stable, and the settling time T_{\max} is estimated by

$$T(e(t_0)) \leq T_{\max} = \frac{1}{b^k} \left(\frac{b}{a}\right)^{\frac{1}{\eta}} \left(1 + \frac{1}{\eta k - 1}\right)$$

Lemma 2. (see³¹) Let $a_1, a_2, \dots, a_N, p > 1$, then the following inequality hold

$$\sum_{i=1}^N a_i^p \geq N^{1-p} \left(\sum_{i=1}^N a_i\right)^p$$

Lemma 3. (see³²) Assume that a continuous, positive-definite function $V(e(t))$ satisfies the following differential inequality:

$$\dot{V}(e(t)) + \alpha V^\eta(e(t)) \leq 0, \quad \forall t \geq t_0, \quad V(e(t_0)) \geq 0,$$

where $\alpha > 0, 0 < \eta < 1$ are two constants. Then, for any given $t_0, V(e(t))$ satisfies the following differential inequality:

$$V^{1-\eta}(e(t)) \leq V^{1-\eta}(e(t_0)) - \alpha(1-\eta)(t-t_0), t_0 \leq t \leq t_1,$$

and

$$V(e(t)) \equiv 0, \forall t \geq t_1,$$

with t_1 given by

$$t_1 = t_0 + \frac{V^{1-\eta}(t_0)}{\alpha(1-\eta)}.$$

Denote

$$\bar{a}_{kq} = \max\{\hat{a}_{kq}, \check{a}_{kq}\}, \underline{a}_{kq} = \min\{\hat{a}_{kq}, \check{a}_{kq}\}.$$

$$\bar{b}_{kq} = \max\{\hat{b}_{kq}, \check{b}_{kq}\}, \underline{b}_{kq} = \min\{\hat{b}_{kq}, \check{b}_{kq}\}.$$

$$a_{kq} = \frac{1}{2}(\bar{a}_{kq} + \underline{a}_{kq}), \tilde{a}_{kq} = \frac{1}{2}(\bar{a}_{kq} - \underline{a}_{kq}).$$

$$b_{kq} = \frac{1}{2}(\bar{b}_{kq} + \underline{b}_{kq}), \tilde{b}_{kq} = \frac{1}{2}(\bar{b}_{kq} - \underline{b}_{kq}).$$

The Eq.(1) and Eq.(4) can be written as

$$\begin{aligned} \dot{x}_{ik}(t) &\in -c_k x_{ik}(t) + \sum_{q=1}^n (a_{kq} + \bar{c}o[-\tilde{a}_{kq}, \tilde{a}_{kq}]) \bar{g}_q(x_{ik}(t)) \\ &+ \sum_{q=1}^n (b_{kq} + \bar{c}o[-\tilde{b}_{kq}, \tilde{b}_{kq}]) g_q(x_{ik}(t - \tau_0)) \\ &+ \sigma \sum_{j=1}^N w_{ij}^0 \gamma_k x_{jk}(t) \\ &+ \sigma \sum_{l=1}^m \sum_{j=1}^N w_{ij}^l \gamma_k x_{jk}(t - \tau_l) + I_i(t), \end{aligned} \tag{5}$$

$$\begin{aligned}
\dot{y}_{ik}(t) \in & -c_k y_{ik}(t) + \sum_{q=1}^n (a_{kq} + \bar{c}\bar{o}[-\tilde{a}_{kq}, \tilde{a}_{kq}]) \bar{g}_q(y_{ik}(t)) \\
& + \sum_{q=1}^n (b_{kq} + \bar{c}\bar{o}[-\tilde{b}_{kq}, \tilde{b}_{kq}]) g_q(y_{ik}(t - \tau_0)) \\
& + \sigma \sum_{j=1}^N w_{ij}^0 \gamma_k y_{jk}(t) \\
& + \sigma \sum_{l=1}^m \sum_{j=1}^N w_{ij}^l \gamma_k y_{jk}(t - \tau_l) + I_i(t) + u_{ik}(t),
\end{aligned} \tag{6}$$

Remark 2. According to the state-dependence conditions of Eqs.(5) and (6), the variables $\bar{c}\bar{o}[-\tilde{a}_{kq}, \tilde{a}_{kq}]$, $\bar{c}\bar{o}[-\tilde{b}_{kq}, \tilde{b}_{kq}]$ may not reach their maximum and minimum values at the same time. Therefore, we give the follow four different measurable functions to represent interval information.

According to the measurable selection theorem [34], there exist measurable functions $\xi_{kq}^1(t), \xi_{kq}^2(t), \xi_{kq}^3(t), \xi_{kq}^4(t) \in \bar{c}\bar{o}[-1, 1]$ such that

$$\begin{aligned}
\dot{x}_{ik}(t) = & -c_k x_{ik}(t) + \sum_{q=1}^n (a_{kq} + \tilde{a}_{kq} \xi_{kq}^1(t)) \bar{g}_q(x_{ik}(t)) \\
& + \sum_{q=1}^n (b_{kq} + \tilde{b}_{kq} \xi_{kq}^3(t)) g_q(x_{ik}(t - \tau_0)) \\
& + \sigma \sum_{j=1}^N w_{ij}^0 \gamma_k x_{jk}(t) \\
& + \sigma \sum_{l=1}^m \sum_{j=1}^N w_{ij}^l \gamma_k x_{jk}(t - \tau_l) + I_i(t),
\end{aligned} \tag{7}$$

$$\begin{aligned}
\dot{y}_{ik}(t) = & -c_k y_{ik}(t) + \sum_{q=1}^n (a_{kq} + \tilde{a}_{kq} \xi_{kq}^2(t)) \bar{g}_q(y_{ik}(t)) \\
& + \sum_{q=1}^n (b_{kq} + \tilde{b}_{kq} \xi_{kq}^4(t)) g_q(y_{ik}(t - \tau_0)) \\
& + \sigma \sum_{j=1}^N w_{ij}^0 \gamma_k y_{jk}(t) \\
& + \sigma \sum_{l=1}^m \sum_{j=1}^N w_{ij}^l \gamma_k y_{jk}(t - \tau_l) + I_i(t) + u_{ik}(t),
\end{aligned} \tag{8}$$

Let $e_{ik}(t) = y_{ik}(t) - x_{ik}(t)$, the corresponding error system is given as follows:

$$\begin{aligned}
\dot{e}_{ik}(t) = & -c_k e_{ik}(t) + \sum_{q=1}^n a_{kq} (\bar{g}_q(y_{ik}(t)) - \bar{g}_q(x_{ik}(t))) \\
& + \sum_{q=1}^n \tilde{a}_{kq} \xi_{kq}^2(t) (\bar{g}_q(y_{ik}(t)) - \bar{g}_q(x_{ik}(t))) \\
& + \sum_{q=1}^n \tilde{a}_{kq} (\xi_{kq}^2(t) - \xi_{kq}^1(t)) \bar{g}_q(x_{ik}(t)) \\
& + \sum_{q=1}^n b_{kq} (g_q(y_{ik}(t - \tau_0)) - g_q(x_{ik}(t - \tau_0))) \\
& + \sum_{q=1}^n \tilde{b}_{kq} \xi_{kq}^4(t) (\bar{g}_q(y_{ik}(t)) - \bar{g}_q(x_{ik}(t))) \\
& + \sum_{q=1}^n \tilde{b}_{kq} (\xi_{kq}^4(t) - \xi_{kq}^3(t)) \bar{g}_q(x_{ik}(t)) \\
& + \sigma \sum_{j=1}^N w_{ij}^0 \gamma_k e_{jk}(t) + \sigma \sum_{l=1}^m \sum_{j=1}^N w_{ij}^l \gamma_k e_{jk}(t - \tau_l) + u_{ik}(t),
\end{aligned} \tag{9}$$

Remark 3. Based on the Definition 2, the issues of fixed-time synchronization between the drive system (1) and response system (4) are transformed into the issues of fixed-time stability of error system (9).

3 | FIXED-TIME SYNCHRONIZATION FOR MCMNN

In order to guarantee the fixed-time synchronization of drive-response systems, the controller is designed as follows:

$$u_{ik} = -\alpha_i e_{ik}(t) - \text{sign}(e_{ik}(t))(\beta_i + \sum_{l=0}^m r_l |e_{ik}(t - \tau_l)| + \delta_i |e_{ik}|^\eta), \quad (10)$$

where $i = 1, 2, \dots, N, k = 1, 2, \dots, n$. $\alpha_i, \beta_i, r_i \geq 0$ and $\delta_i \geq 1$. And $\text{sign}(x)$ is the sign function which is defined as follows:

$$\text{sign}(x) = \begin{cases} -1, & \text{if } x < 0, \\ 0, & \text{if } x = 0, \\ 1, & \text{if } x > 0. \end{cases}$$

According to Assumptions 1 and 2, combined with the designed controller (10), we obtain

$$\begin{aligned} \dot{e}_{ik}(t) \leq & -c_k e_{ik}(t) + \sum_{q=1}^n a_{kq} \bar{f}_q |e_{ik}(t)| \\ & + \sum_{q=1}^n \tilde{a}_{kq} \xi_{kq}^2(t) \bar{f}_q |e_{ik}(t)| + 2 \sum_{q=1}^n \tilde{a}_{kq} \bar{M}_q \\ & + \sum_{q=1}^n b_{kq} f_q |e_{ik}(t - \tau_0)| \\ & + \sum_{q=1}^n \tilde{b}_{kq} \xi_{kq}^4(t) f_q |e_{ik}(t - \tau_0)| + 2 \sum_{q=1}^n \tilde{b}_{kq} M_q \\ & + \sigma \sum_{j=1}^N w_{ij}^0 \gamma_k e_{jk}(t) + \sigma \sum_{l=1}^m \sum_{j=1}^N w_{ij}^l \gamma_k e_{jk}(t - \tau_l) \\ & - \alpha_i e_{ik}(t) - \text{sign}(e_{ik}(t))(\beta_i + \sum_{l=0}^m r_l |e_{ik}(t - \tau_l)| + \delta_i |e_{ik}|^\eta), \end{aligned} \quad (11)$$

Based on the designed controller (10) applied on the response system, a theorem is presented to achieve the fixed-time synchronization for MCMNN.

Denote $\gamma_{\max} = \max_{1 \leq k \leq n} (\gamma_k), \alpha = \text{diag}(\alpha_1, \alpha_2, \dots, \alpha_N), \beta = \text{diag}(\beta_1, \beta_2, \dots, \beta_N),$

$r = \text{diag}(r_1, r_2, \dots, r_N), W_l = (w_{ij}^l)_{N \times N}, l = 1, 2, \dots, m.$

$\phi_1 = \max_{1 \leq k \leq n} \{-c_k + \sum_{q=1}^n (a_{kq} + \tilde{a}_{kq}) \bar{f}_q\}, \phi_2 = \max_{1 \leq k \leq n} \{\sum_{q=1}^n (b_{kq} + \tilde{b}_{kq}) f_q\},$

$\phi_3 = \max_{1 \leq k \leq n} \{2 \sum_{q=1}^n (\tilde{a}_{kq} \bar{M}_q + \tilde{B}_{kq} M_q)\}$

Theorem 1. Under Assumptions 1,2 and the controller (10), the error system (9) is fixed-time stable if

$$\begin{cases} \phi_1 I_N - \alpha + \sigma \gamma_{\max} W_0 \leq 0, \\ \phi_2 I_N - (m+1)r + \sigma \gamma_{\max} \sum_{l=1}^m W_l \leq 0, \\ \phi_3 I_N - \beta \leq 0. \end{cases}$$

Then, the setting time can be obtained by approximate formula

$$T(e(t_0)) \leq T_{\max} = \frac{\eta}{\theta(\eta-1)} \left(\frac{\theta}{\lambda n^{1-\eta}} \right)^{\frac{1}{\eta}},$$

where $\lambda = \min_{1 \leq i \leq N} \{\delta_i\}, \theta = \min_{1 \leq i \leq N} (\beta - \phi_3).$

We construct a Lyapunov function as follows:

$$V(e(t)) = \sum_{i=1}^N |e_i(t)| = \sum_{i=1}^N \sum_{k=1}^n |e_{ik}(t)|.$$

Then, the derivative of $V(e(t))$ is along the trajectories of $e(t)$. we have

$$\begin{aligned}
\dot{V}(e(t)) &= \sum_{i=1}^N \sum_{k=1}^n \text{sign}(e_{ik}(t)) \dot{e}_{ik}(t), \\
&\leq \sum_{i=1}^N \sum_{k=1}^n -c_k |e_{ik}(t)| + \sum_{i=1}^N \sum_{k=1}^n \sum_{q=1}^n (a_{kq} + \tilde{a}_{kq}) \bar{f}_q |e_{ik}(t)| \\
&\quad + \sum_{i=1}^N \sum_{k=1}^n \sum_{q=1}^n (b_{kq} + \tilde{b}_{kq}) f_q |e_{ik}(t - \tau_0)| \\
&\quad + 2 \sum_{i=1}^N \sum_{k=1}^n \sum_{q=1}^n (\tilde{a}_{kq} \bar{M}_q + \tilde{b}_{kq} M_q) \\
&\quad + \sigma \sum_{i=1}^N \sum_{j=1}^N \sum_{k=1}^n w_{ji}^0 \gamma_k |e_{ik}(t)| + \sigma \sum_{i=1}^N \sum_{j=1}^N \sum_{k=1}^n \sum_{l=1}^m w_{ji}^l \gamma_k |e_{ik}(t - \tau_l)| \\
&\quad - \sum_{i=1}^N \sum_{k=1}^n \alpha_i |e_{ik}(t)| - \sum_{i=1}^N \sum_{k=1}^n \beta_i - \sum_{i=1}^N \sum_{k=1}^n \sum_{l=0}^m r_i |e_{ik}(t - \tau_l)| - \sum_{i=1}^N \sum_{k=1}^n \delta_i |e_{ik}|^\eta, \\
&\leq \sum_{i=1}^N \sum_{k=1}^n [-c_k + \sum_{q=1}^n (a_{kq} + \tilde{a}_{kq}) \bar{f}_q + \sigma \sum_{j=1}^N w_{ji}^0 \gamma_{\max} - \alpha_i] |e_{ik}(t)| \\
&\quad + \sum_{i=1}^N \sum_{k=1}^n \sum_{q=1}^n [\sum_{l=1}^m (b_{kq} + \tilde{b}_{kq}) f_q - r_i] |e_{ik}(t - \tau_0)| \\
&\quad + \sum_{i=1}^N \sum_{k=1}^n \sum_{l=1}^m (\sigma \sum_{j=1}^N w_{ji}^l \gamma_{\max} - r_i) |e_{ik}(t - \tau_l)| \\
&\quad - \sum_{i=1}^N \sum_{k=1}^n [\beta_i - 2 \sum_{q=1}^n (\tilde{a}_{kq} \bar{M}_q + \tilde{b}_{kq} M_q)] \\
&\quad - \sum_{i=1}^N \sum_{k=1}^n \delta_i |e_{ik}|^\eta, \\
&\leq - \sum_{i=1}^N \sum_{k=1}^n \delta_i |e_{ik}|^\eta - \sum_{i=1}^N \sum_{k=1}^n [\beta_i - 2 \sum_{q=1}^n (\tilde{a}_{kq} \bar{M}_q + \tilde{b}_{kq} M_q)],
\end{aligned}$$

Let $\lambda = \min_{1 \leq i \leq N} \{\delta_i\}$, $\theta = \min_{1 \leq i \leq N} (\beta_i - \phi_3)$, and by Lemma 2, we obtain

$$\dot{V}(e(t)) \leq -\lambda n^{1-\eta} (V(e(t)))^\eta - \theta.$$

According to Lemma 1 and $k = 1$, the settling time is obtain as follows:

$$T(e(t_0)) \leq T_{max} = \frac{\eta}{\theta(\eta - 1)} \left(\frac{\theta}{\lambda n^{1-\eta}} \right)^{\frac{1}{\eta}}$$

The proof of Theorem 1 is completed.

Remark 4. Based on the Definition 2, Lemmas 2 and 3, the error system is said to achieve to the fixed-time stable if it is the finite-time stable and there exist the settling time $T(e_0)$ such that $T(e_0) \leq T_{max}$, $\forall e_0 \in R^n$. Therefore, the error system (9) can achieve the finite-time stable based on the above controller (10).

Corollary 1. Under Assumptions 1,2 and the controller (10), the drive-response systems (1) and (4) can achieve the finite-time synchronization if

$$\begin{cases} \phi_1 I_N - \alpha + \sigma \gamma_{max} W_0 \leq 0, \\ \phi_2 I_N - (m + 1)r + \sigma \gamma_{max} \sum_{l=1}^m W_l \leq 0, \\ \phi_3 I_N - \beta \leq 0. \end{cases}$$

We also construct the same Lyapunov function as follows:

$$V(e(t)) = \sum_{i=1}^N |e_i(t)| = \sum_{i=1}^N \sum_{k=1}^n |e_{ik}(t)|.$$

Then, the derivative of $V(e(t))$ without parameter θ is along the trajectories of $e(t)$ is written as:

$$\dot{V}(e(t)) + \sum_{i=1}^N \delta_i |e_i|^\eta \leq 0.$$

Then, the finite-time can be obtained as follows:

$$t_0 = \frac{V(0)^{1-\eta}}{\delta(1-\eta)}.$$

The results of Theorem 1 can also easily extend to the general single coupled memristive neural network which does not multi-links items. The drive-response systems are given as

$$\left\{ \begin{array}{l} \dot{x}_{ik}(t) = -c_k x_{ik}(t) + \sum_{q=1}^n a_{kq}(x_{ik}(t)) \bar{g}_q(x_{ik}(t)) \\ \quad + \sum_{q=1}^n b_{kq}(x_{ik}(t - \tau_0)) g_q(x_{ik}(t - \tau_0)) \\ \quad + \sigma \sum_{j=1}^N w_{ij}^0 \Gamma x_{jk}(t) + I_i, \\ \dot{y}_{ik}(t) = -c_k y_{ik}(t) + \sum_{q=1}^n a_{kq}(y_{ik}(t)) \bar{g}_q(y_{ik}(t)) \\ \quad + \sum_{q=1}^n b_{kq}(y_{ik}(t - \tau_0)) g_q(y_{ik}(t - \tau_0)) \\ \quad + \sigma \sum_{j=1}^N w_{ij}^0 \Gamma y_{jk}(t) + I_i + u_{ik}(t). \end{array} \right. \quad (12)$$

the controller is designed as follows:

$$u_{ik} = -\alpha_i e_{ik}(t) - \text{sign}(e_{ik}(t))(\beta_i + r_i |e_{ik}(t - \tau_0)| + \delta_i |e_{ik}|^\eta), \quad (13)$$

According to the drive-response system (12), the corresponding corollary is given as

Corollary 2. Under Assumptions 1,2 and the controller (13), the drive-response systems (12) can achieve the fixed-time synchronization if

$$\left\{ \begin{array}{l} \phi_1 I_N - \alpha + \sigma \gamma_{max} W_0 \leq 0, \\ \phi_2 I_N - r \leq 0, \\ \phi_3 I_N - \beta \leq 0. \end{array} \right.$$

The results of Theorem 1 can also further extend to the general memristive neural network which does not coupled topology. The drive-response systems are given as

$$\left\{ \begin{array}{l} \dot{x}_{ik}(t) = -c_k x_{ik}(t) + \sum_{q=1}^n a_{kq}(x_{ik}(t)) \bar{g}_q(x_{ik}(t)) \\ \quad + \sum_{q=1}^n b_{kq}(x_{ik}(t - \tau_0)) g_q(x_{ik}(t - \tau_0)) + I_i \\ \dot{y}_{ik}(t) = -c_k y_{ik}(t) + \sum_{q=1}^n a_{kq}(y_{ik}(t)) \bar{g}_q(y_{ik}(t)) \\ \quad + \sum_{q=1}^n b_{kq}(y_{ik}(t - \tau_0)) g_q(y_{ik}(t - \tau_0)) + I_i + u_{ik}(t). \end{array} \right. \quad (14)$$

According to the drive-response system (14), we give the corresponding corollary as follows:

Corollary 3. Under Assumptions 1,2 and the controller (13), the drive-response systems (14) can achieve the fixed-time synchronization if

$$\left\{ \begin{array}{l} \phi_1 I_n - \alpha \leq 0, \\ \phi_2 I_n - r \leq 0, \\ \phi_3 I_n - \beta \leq 0. \end{array} \right.$$

4 | DESIGN OF SECURE COMMUNICATION SCHEME

The section give a secure communication scheme based on the fixed-time synchronous control of MCMNN, which comprises the following steps:

Step 1: The three-dimensional drive-response systems $x_i(t)$ and $y_i(t)$ are builded, which are respectively MCMNN;
 Step 2: According to drive-response systems, the synchronization error system $e_i(t) = y_i(t) - x_i(t)$ is established;
 Step 3: The fixed-time stability theorem (Theorem 1) with low conservation is adopted;
 Step 4: The appropriate fixed-time synchronization controller $u_i(t)$ is designed;
 Step 5: A new fixed-time synchronization control theorem is given to realize the fixed-time stability of the error system, and the more accurate upper bound of the stable time T_{\max} is calculated;
 Step 6: The implementation of secure communication scheme:

Sender: the mixed signal generated by the plaintext signal and the prefixed random signal is introduced into the drive system of coupled memristive neural network with multi-links, and the sender generates encrypted signal by superimposing the drive system signal and mixed signal, and sends it to the receiver through the transmission channel.

The designed plaintext signals without any encrypt are $m_i(t)$, $i = 1, 2, 3$.

The mixed signal by the plaintext signals and random signal are given as

$$M_i(t) = \begin{cases} r_i(t), 0 \leq t < T_{\max}, \\ m_i(t - T_{\max}), t \geq T_{\max}. \end{cases}$$

where $i = 1, 2, 3$.

Remark 4. The used of random signal before encrypted signal is to enhance the security of the transmit signals.

The encrypted signal by superimposing the drive system signal and mixed signal are $E_i(t) = M_i(t) + x_i(t)$.

Receiver: the received transmitted signal, the known key and public parameter information are introduced into the response system. The fixed-time stability theorem given by step 3 and the fixed-time synchronization of drive-response systems are realized under the synchronization controller. Through calculation, the receiver can decrypt the plaintext signal.

According to the fixed time T_{\max} , if $t > T_{\max}$, then $x_i(t) = y_i(t)$. The receiver can decrypt the plaintext signal by the following formula:

$$\begin{aligned} m'_i(t) &= E_i(t + T_{\max}) - y_i(t + T_{\max}), \\ &= M_i(t + T_{\max}) + x_i(t + T_{\max}) - y_i(t + T_{\max}), \\ &= M_i(t + T_{\max}) \\ &= m_i(t), t \geq 0. \end{aligned}$$

Note: The sender and the receiver have a common key; all parameters of the drive system generated by the sender are public; after generating the drive system, the sender destroys the initial value of the system and cannot be disclosed.

The predetermined fixed time transmission signal and the recovery plaintext signal can improve the transmission efficiency and ensure the security of signal transmission in the secure communication scheme based on the fixed-time synchronous control of MCMNN. This scheme has the following advantages: (1) We can use Simulink in MATLAB to build a three-dimensional MCMNN or program simulation in MATLAB to design a secure communication scheme based on fixed-time synchronous control of drive-response systems, and the design scheme is flexible. (2) In the secure communication scheme, the encrypted signal superimposed by the three-dimensional system is relatively complex and is not easy to crack. (3) In the secure communication scheme, both the drive system and the response system contain three differential equations, and the secure communication is realized under the synchronous control of the drive-response system, which provides a new perspective for the research of secure communication. (4) The scheme can preset the synchronization time according to the need, and it can predict the communication time more accurately and effectively, and improve the efficiency and security of the transmission information. (5) The secure communication scheme has good expansibility and can be applied to the encrypted transmission of various images, videos and other signals and the abnormal detection system of information.

5 | NUMERICAL SIMULATIONS

Example 1: Consider the following three-neuron CMNN with three-links as drive-response systems:

$$\left\{ \begin{array}{l} \dot{x}_{ik}(t) = -c_k x_{ik}(t) + a_{kq}(x_{ik}(t))\bar{g}(x_{ik}(t)) \\ \quad + b_{kq}(x_{ik}(t - \tau_0))g(x_{ik}(t - \tau_0)) \\ \quad + \sigma \sum_{j=1}^N w_{ij}^0 \Gamma x_{jk}(t) \\ \quad + \sigma \sum_{j=1}^N w_{ij}^1 \Gamma x_{jk}(t - \tau_1) \\ \quad + \sigma \sum_{j=1}^N w_{ij}^2 \Gamma x_{jk}(t - \tau_2) + I_i(t), \\ \dot{y}_{ik}(t) = -c_k y_{ik}(t) + a_{kq}(y_{ik}(t))\bar{g}(y_{ik}(t)) \\ \quad + b_{kq}(y_{ik}(t - \tau_0))g(y_{ik}(t - \tau_0)) \\ \quad + \sigma \sum_{j=1}^N w_{ij}^0 \Gamma y_{jk}(t) \\ \quad + \sigma \sum_{j=1}^N w_{ij}^1 \Gamma y_{jk}(t - \tau_1) \\ \quad + \sigma \sum_{j=1}^N w_{ij}^2 \Gamma y_{jk}(t - \tau_2) + I_i(t) + u_i(t), \end{array} \right. \quad (15)$$

where $i = 1, 2, \dots, 8$, $c = \text{diag}(5, 6, 7)$, $N = 8$, $\sigma = 1$, $\Gamma = I_{3 \times 3}$. $I_i(t)$ can be omit in the simulation. The active functions $\bar{g}(x) = \frac{1}{2}(|x+1| - |x-1|) - 1$, $g(x) = \frac{1}{4}(|x+1| - |x-1|)$. The time-delays are $\tau_0 = 0.1$, $\tau_1 = 0.2$, $\tau_2 = 0.4$. The configuration matrices W_l , $l = 0, 1, 2$ are given by

$$W_0 = \begin{bmatrix} -5 & 1 & 1 & 0 & 1 & 1 & 1 & 0 \\ 1 & -5 & 0 & 1 & 1 & 1 & 0 & 1 \\ 1 & 0 & -4 & 1 & 0 & 0 & 1 & 1 \\ 0 & 1 & 1 & -4 & 1 & 0 & 1 & 0 \\ 1 & 1 & 0 & 1 & -6 & 1 & 1 & 1 \\ 1 & 1 & 0 & 0 & 1 & -3 & 0 & 0 \\ 1 & 0 & 1 & 1 & 1 & 0 & -5 & 1 \\ 0 & 1 & 0 & 0 & 1 & 0 & 1 & -4 \end{bmatrix},$$

$$W_1 = \begin{bmatrix} -4 & 0 & 0 & 1 & 1 & 0 & 1 & 1 \\ 0 & -2 & 1 & 1 & 0 & 0 & 0 & 0 \\ 0 & 1 & -4 & 1 & 1 & 1 & 0 & 0 \\ 1 & 1 & 1 & -3 & 0 & 0 & 0 & 0 \\ 1 & 0 & 1 & 0 & -4 & 1 & 0 & 1 \\ 0 & 0 & 1 & 0 & 1 & -2 & 0 & 0 \\ 1 & 0 & 0 & 0 & 0 & 0 & -1 & 0 \\ 1 & 0 & 0 & 0 & 1 & 0 & 0 & -2 \end{bmatrix},$$

$$W_2 = \begin{bmatrix} -1 & 1 & 0 & 0 & 0 & 0 & 0 & 0 \\ 1 & -2 & 0 & 1 & 0 & 0 & 0 & 0 \\ 0 & 0 & 0 & 0 & 0 & 0 & 0 & 0 \\ 0 & 1 & 0 & -3 & 1 & 0 & 0 & 1 \\ 0 & 0 & 0 & 1 & -3 & 1 & 0 & 1 \\ 0 & 0 & 0 & 0 & 1 & -1 & 0 & 0 \\ 0 & 0 & 0 & 0 & 0 & 0 & 0 & 0 \\ 0 & 0 & 0 & 1 & 1 & 0 & 0 & -2 \end{bmatrix}.$$

The weight parameters are given by

$$\begin{aligned}
a_{11}(x_{i1}) &= \begin{cases} -0.8, |x_{i1}(t)| \leq 1, \\ -1, |x_{i1}(t)| > 1, \end{cases} & a_{12}(x_{i1}) &= \begin{cases} 2.2, |x_{i1}(t)| \leq 1, \\ 2, |x_{i1}(t)| > 1, \end{cases} & a_{13}(x_{i1}) &= \begin{cases} -1.2, |x_{i1}(t)| \leq 1, \\ 1.8, |x_{i1}(t)| > 1, \end{cases} \\
a_{21}(x_{i2}) &= \begin{cases} 1, |x_{i2}(t)| \leq 1, \\ 0.8, |x_{i2}(t)| > 1, \end{cases} & a_{22}(x_{i2}) &= \begin{cases} -1, |x_{i2}(t)| \leq 1, \\ -0.8, |x_{i2}(t)| > 1, \end{cases} & a_{23}(x_{i2}) &= \begin{cases} -2.4, |x_{i2}(t)| \leq 1, \\ -2, |x_{i2}(t)| > 1, \end{cases} \\
a_{31}(x_{i3}) &= \begin{cases} 0.2, |x_{i3}(t)| \leq 1, \\ 0.4, |x_{i3}(t)| > 1, \end{cases} & a_{32}(x_{i3}) &= \begin{cases} -0.6, |x_{i3}(t)| \leq 1, \\ -0.4, |x_{i3}(t)| > 1, \end{cases} & a_{33}(x_{i3}) &= \begin{cases} -1.8, |x_{i3}(t)| \leq 1, \\ 1.2, |x_{i3}(t)| > 1, \end{cases} \\
b_{11}(x_{i1}) &= \begin{cases} -3.2, |x_{i1}(t-\tau_0)| \leq 1, \\ -3, |x_{i1}(t-\tau_0)| > 1, \end{cases} & b_{12}(x_{i1}) &= \begin{cases} 0.2, |x_{i1}(t-\tau_0)| \leq 1, \\ 0.4, |x_{i1}(t-\tau_0)| > 1, \end{cases} & b_{13}(x_{i1}) &= \begin{cases} 1, |x_{i1}(t-\tau_0)| \leq 1, \\ 1.5, |x_{i1}(t-\tau_0)| > 1, \end{cases} \\
b_{21}(x_{i2}) &= \begin{cases} 0.4, |x_{i2}(t-\tau_0)| \leq 1, \\ 0.2, |x_{i2}(t-\tau_0)| > 1, \end{cases} & b_{22}(x_{i2}) &= \begin{cases} -3.6, |x_{i2}(t-\tau_0)| \leq 1, \\ -3.2, |x_{i2}(t-\tau_0)| > 1, \end{cases} & b_{23}(x_{i2}) &= \begin{cases} 1.5, |x_{i2}(t-\tau_0)| \leq 1, \\ 2.1, |x_{i2}(t-\tau_0)| > 1, \end{cases} \\
b_{31}(x_{i3}) &= \begin{cases} 2.2, |x_{i3}(t-\tau_0)| \leq 1, \\ 2.6, |x_{i3}(t-\tau_0)| > 1, \end{cases} & b_{32}(x_{i3}) &= \begin{cases} 3.2, |x_{i3}(t-\tau_0)| \leq 1, \\ 2.8, |x_{i3}(t-\tau_0)| > 1, \end{cases} & b_{33}(x_{i3}) &= \begin{cases} -2.6, |x_{i3}(t-\tau_0)| \leq 1, \\ 2.4, |x_{i3}(t-\tau_0)| > 1, \end{cases}
\end{aligned}$$

The controller is designed as

$$u_{ik} = -\alpha_i e_{ik}(t) - \text{sign}(e_{ik}(t))(\beta_i + \sum_{l=0}^2 e_{ik}(t - \tau_l) + \delta_i |e_{ik}(t)|^\eta). \quad (16)$$

where $\eta = 1.5 > 1$, the remainder parameters are given by

$$\alpha = \begin{bmatrix} 2 & 3 & 4 \\ 2 & 3 & 4 \\ 2 & 3 & 4 \\ 2 & 3 & 4 \\ 2 & 3 & 4 \\ 2 & 3 & 4 \\ 2 & 3 & 4 \\ 2 & 3 & 4 \end{bmatrix}, \beta = \begin{bmatrix} 1 & 1 & 1 \\ 1 & 1 & 1 \\ 1 & 1 & 1 \\ 1 & 1 & 1 \\ 1 & 1 & 1 \\ 1 & 1 & 1 \\ 1 & 1 & 1 \\ 1 & 1 & 1 \end{bmatrix}, r = \begin{bmatrix} 1 & 1 & 1 \\ 1 & 1 & 1 \\ 1 & 1 & 1 \\ 1 & 1 & 1 \\ 1 & 1 & 1 \\ 1 & 1 & 1 \\ 1 & 1 & 1 \\ 1 & 1 & 1 \end{bmatrix}, \delta = \begin{bmatrix} 8 & 8 & 8 \\ 8 & 8 & 8 \\ 8 & 8 & 8 \\ 8 & 8 & 8 \\ 8 & 8 & 8 \\ 8 & 8 & 8 \\ 8 & 8 & 8 \\ 8 & 8 & 8 \end{bmatrix},$$

The initial values of drive-response systems (14) are given by:

$$x(0) = [5 + i, 1 + 3i, 2 + 5i], y(0) = [2 + 4i, -2 + 4i, 3 + 4i], i = 1, 2, \dots, 8.$$

Figures 2 and 3 describe the phase curves of drive-response system in three dimensional neurons without controller. Figure 4 shows the error state trajectory of drive-response systems (14) without controller. Figure 5 describe the phase curves of drive-response system in three dimensional neurons with controller. Figure 6 shows the error state trajectory of drive-response systems (14) with controller (15).

Using the parameters of the controller (15), we have $\lambda = 1, \theta = 3, \eta = 1.5$, we calculate the settling time $T_{\max} = 3.0$.

Example 2: In this example, we give the secure communication scheme based on the fixed-time synchronization of drive-response systems. Figure 7 show that the schematic diagram of the proposed secure communication scheme. It is worth noting that the transmitted signals are superimposed on a single point three-dimensional neuron of the MCMNN. We consider the following MCMNN of single point form as drive system:

$$\begin{aligned}
\dot{x}_{1i}(t) &= -c_i x_{1i}(t) + \sum_{q=1}^n a_{iq}(x_{1i}(t)) \bar{g}_q(x_{1i}(t)) \\
&+ \sum_{q=1}^n b_{iq}(x_{1i}(t - \tau_0)) g_q(x_{1i}(t - \tau_0)) \\
&+ \sigma \sum_{j=1}^N w_{1j}^0 \Gamma x_{ji}(t) \\
&+ \sigma \sum_{l=1}^m \sum_{j=1}^N w_{1j}^l \Gamma x_{ji}(t - \tau_l),
\end{aligned} \quad (17)$$

where

$$M_i(t) = \begin{cases} r_i(t), 0 \leq t < 3, \\ m_i(t-3), t \geq 3. \end{cases}$$

$$\begin{cases} r_1(t) = \text{rand}(-1, 1), \\ r_2(t) = \text{rand}(-3, 3), \\ r_3(t) = \text{rand}(-2, 2), \end{cases} \begin{cases} m_1(t) = 0.5 \sin(2t) + 0.3 \cos(0.5t), \\ m_2(t) = -\sin(3t) + 2 \cos(1.2t), \\ m_3(t) = \sin(3t) - 2 \cos(3t). \end{cases}$$

The remainder parameters are given as same as the Example 1. Figures 8-11 illustrate the state trajectories of $x_{1i}(t), m_i(t), M_i(t)$ and $E_i(t), i = 1, 2, 3$. The initial values of drive system (17), $m_i(t), r_i(t)$ and $M_i(t)$ can only be known by sender. The common keys of sender and receiver are c_i, T_i and the calculated T_{\max} . After the receiver receives the secret keys and the encrypted signal $E_i(t), i = 1, 2, 3$, the receiver generates the response system as follows:

$$\begin{aligned} \dot{y}_{1i}(t) = & -c_i y_{1i}(t) + \sum_{q=1}^n a_{iq}(y_{1i}(t)) \bar{g}_q(y_{1i}(t)) \\ & + \sum_{q=1}^n b_{iq}(y_{1i}(t - \tau_0)) g_q(y_{1i}(t - \tau_0)) \\ & + \sigma \sum_{j=1}^N w_{1j}^0 \Gamma y_{ji}(t) \\ & + \sigma \sum_{l=1}^m \sum_{j=1}^N w_{1j}^l \Gamma y_{ji}(t - \tau_l) + u_i(t), \end{aligned} \quad (18)$$

where the parameters are given as same as the Example 1 too. Since $T_{\max} = 3$, we have $x_{1i}(t) = y_{1i}(t), i = 1, 2, 3, t \geq 3$. Receiver can decrypted the encrypted signal by calculated the following formula:

$$\begin{aligned} m'_i(t) &= E_i(t+3) - y_{1i}(t+3), \\ &= M_i(t+3) + x_{1i}(t+3) - y_{1i}(t+3), \\ &= M_i(t+3) \\ &= m_i(t), t \geq 0. \end{aligned}$$

Figure 12 illustrates the state trajectories of error system under the controller.

6 | CONCLUSIONS

We investigated the fixed-time synchronization of coupled memristive neural networks with multi-links, coupled forms and multi-links performance increase the complexity and the unstable of systems. The fixed-time stability theorem and the effective controller are given to guarantee fixed-time synchronization of drive-response systems based on differential inclusion theory and the concept of set-valued mapping. Further, we designed an effective secure communication scheme based on fixed-time synchronization of drive-response systems. Undeniably, compared with some mature secure communication schemes, the secure communication schemes in this section are also relatively shallow. However, the related research results are expected to provide a new perspective for the research of secure communication. Finally, numerical simulation of fixed-time synchronization and an example of secure communication are show to verify the effectiveness of theoretical research. In the future, The more expansibility secure communication scheme based on the fixed-time stability are designed to apply to optimize encryption and selective encryption scheme needed by people.

ACKNOWLEDGMENTS

The work is supported by the Shandong Province Natural Science Foundation under Grant no. ZR2018BF023, National Natural Science Foundation of China under Grant Nos. 61701192, 61671242, 61872419, 61873324, 61702307, 61901191 and the Opening fund of National Engineering Laboratory for Transportation Safety & Emergency Informatics under Grant YW170301-07.

References

1. Y Tang, LO Chua. Impulsive stabilization for control and synchronization of chaotic systems: Theory and application to secure communication. *IEEE Transactions on Circuits and Systems I: Fundamental Theory and Applications*. 1977;44(10):976–988.
2. F Moez. An adaptive chaos synchronization scheme applied to secure communication. *Chaos Solitons & Fractals*. 2003;18(1):141–148.
3. R Femat, R Jaureguiortiz, G Solisperales. A chaos-based communication scheme via robust asymptotic feedback. *IEEE Transactions on Circuits & Systems I Fundamental Theory & Applications*. 2004;48(10):1161–1169.
4. G Zheng, D Boutat, Floquet T et al. Secure Communication Based on Multi-input Multi-output Chaotic System with Large Message Amplitude. *Chaos Solitons & Fractals*. 2009;41(3):1510–1517.
5. H Zhao, L Li, H Peng, J Kurths, J Xiao, Y Yang. Anti-synchronization for stochastic memristor-based neural networks with non-modeled dynamics via adaptive control approach. In: :1–10; 2015.
6. S Gong, S Yang, Guo Z et al. Global exponential synchronization of inertial memristive neural networks with time-varying delay via nonlinear controller. In: :138–148; 2018.
7. Z Cai, L Huang. Finite-Time Stabilization of Delayed Memristive Neural Networks: Discontinuous State-Feedback and Adaptive Control Approach. *IEEE Transactions on Neural Networks & Learning Systems*. 2017;99(4):856–868.
8. M Zheng, L Li, Peng H et al. Finite-time stability and synchronization of memristor-based fractional-order fuzzy cellular neural networks. *Communications in Nonlinear Science and Numerical Simulation*. 2018;59:272–291.
9. P Dorato. Short-time stability in linear time-varying system. *Proceedings of the IRE International Convention Record Part*. 1961;4:83–87.
10. A Polyakov. Nonlinear feedback design for fixed-time stabilization of linear control systems. In: 1971 (pp. 2106–2110).
11. LO Chua. Memristor the missing circuit element. *IEEE Transactions on Circuit Theory*. 1971;18:507–519.
12. C Chen, L Li, Peng H et al. *A new fixed-time stability theorem and its application to the fixed-time synchronization of neural networks*. : Los Alamos National Laboratory; 2020.
13. H Zhao, L Li, H Peng, J Xiao, Y Yang, M Zheng. Impulsive control for synchronization and parameters identification of uncertain multi-links complex network. *Nonlinear Dynamics*. 2015;83(3):1–15.
14. J Cao, R Li. Fixed-time synchronization of delayed memristor-based recurrent neural networks. *Science China Information Sciences*. 2017;60(032201):1–15.
15. R Wei, J Cao, A Alsaedi. Fixed-time synchronization of memristive Cohen-Grossberg neural networks with impulsive effects. *International Journal of Control, Automation and Systems*. 2018;16(5):2214–2224.
16. M Zheng, L Li, Peng H et al. Fixed-time synchronization of memristor-based fuzzy cellular neural network with time-varying delay. *Journal of the Franklin Institute*. 2018;355(14):6780–6809.
17. C Chen, L Li, Peng H et al. A new fixed-time stability theorem and its application to the synchronization control of memristive neural networks. *Neurocomputing*. 2019;349(15):290–300.
18. R Wei, J Cao, A Alsaedi. Finite-time and fixed-time synchronization analysis of inertial memristive neural networks with time-varying delays. In: 2018 (pp. 121–134).
19. C Chen, L Li, Peng H et al. Fixed-time synchronization of inertial memristor-based neural networks with discrete delay. *Neural Networks*. 2018;109:81–89.

20. X Haliding, H Jiang, Abdurahman A et al. Fixed-Time Lag Synchronization Analysis for Delayed Memristor-Based Neural Networks. *Neural Processing Letters*. 2020;52:485–509.
21. Y Zhang, J Zhuang, Xia Y et al. *Fixed-time synchronization of the impulsive memristor-based neural networks*. : ; 2019.
22. H Ren, Z Peng, Y Gu. Fixed-time synchronization of stochastic memristor-based neural networks with adaptive control. In: :165–175; 2020.
23. R Wei, J Cao. Fixed-time synchronization of quaternion-valued memristive neural networks with time delays. *Neural Networks*. 2019;113:1–10.
24. C Yang, L Huang, Z Cai. Fixed-time synchronization of coupled memristor-based neural networks with time-varying delays. *Neural Networks*. 2019;116:101–109.
25. S Gong, Z Guo, Wen S et al. *Finite-Time and Fixed-Time Synchronization of Coupled Memristive Neural Networks With Time Delay*. : ; 2019.
26. J Li, H Jiang, Hu C et al. *Finite/Fixed-Time Synchronization Control of Coupled Memristive Neural Networks*. 2019.
27. Y Guo, Y Luo, Wang W et al. Fixed-time Synchronization of Complex-valued Memristive BAM Neural Network and Applications in Image Encryption and Decryption. *International Journal of Control, Automation and Systems*. 2020;18(2):462–476.
28. H Zhao, L Li, H Peng, J Xiao, Y Yang, M Zheng. Finite-time topology identification and stochastic synchronization of complex network with multiple time delays. *Neurocomputing*. 2016;219:39–49.
29. F Filippov A. Differential equations with discontinuous right-hand side. *Matematicheskii Sbornik*. 1960;51(93):99–128.
30. C Hu, J Yu, Chen Z et al. Fixed-time stability of dynamical systems and fixed-time synchronization of coupled discontinuous neural networks. *Neural Networks*. 2017;89:74–83.
31. Khalil HK Grizzle J. *Nonlinear Systems. third ed., Prentice Hall, Upper Saddle River*. 2002;.
32. Y Tang. Terminal sliding mode control for rigid robots. *Automatica*. 1998;34:51–56.



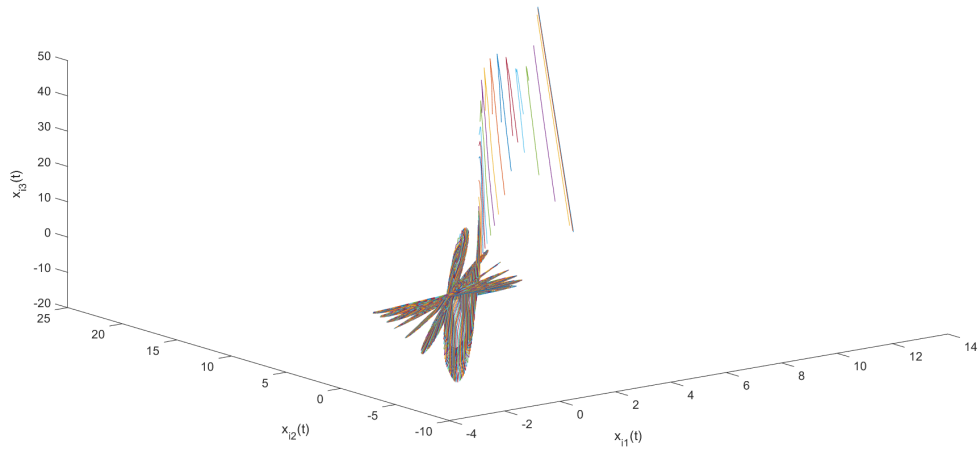


FIGURE 2 The phase curves of drive system in three dimensional neurons.

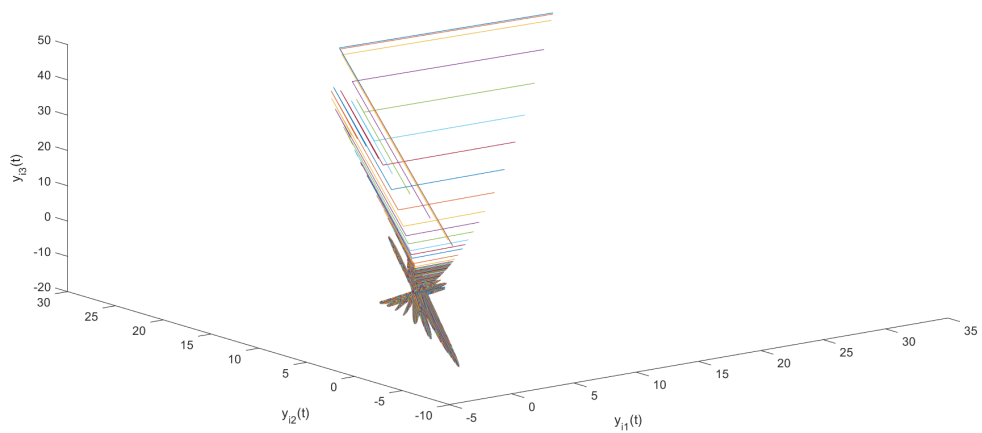


FIGURE 3 The phase curves of response system without the controller in three dimensional neurons.

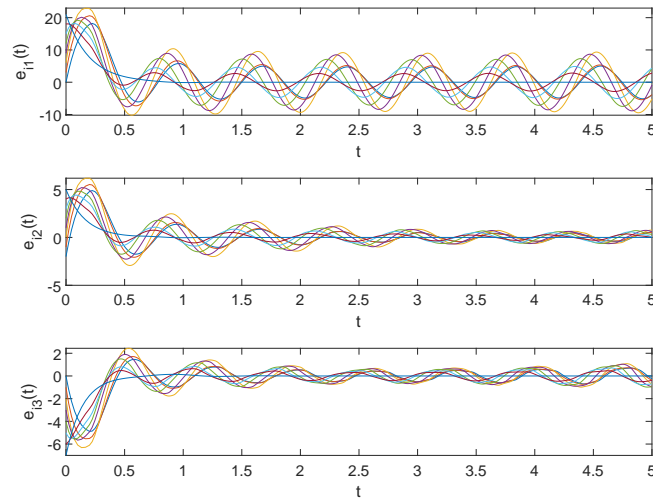


FIGURE 4 The error system of drive-response systems (15) without the controller.

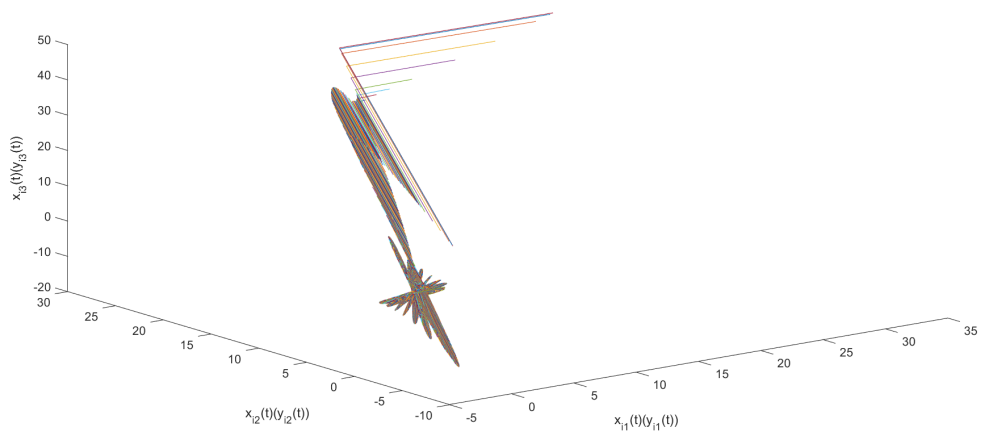


FIGURE 5 The phase curves of drive-response systems (15) with the controller.

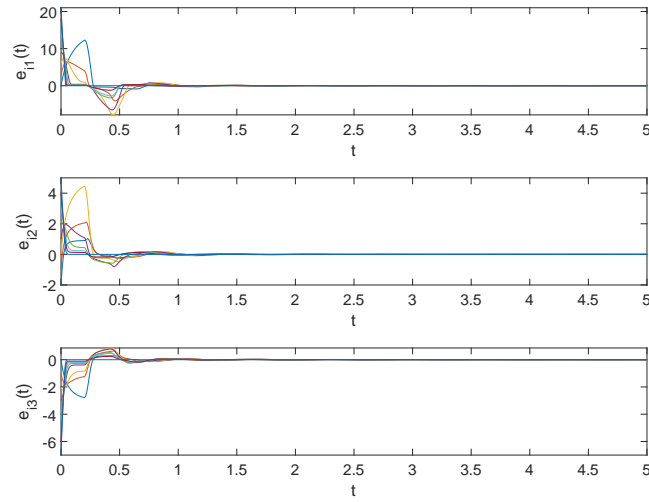


FIGURE 6 The error system of drive-response systems (15) with the controller.

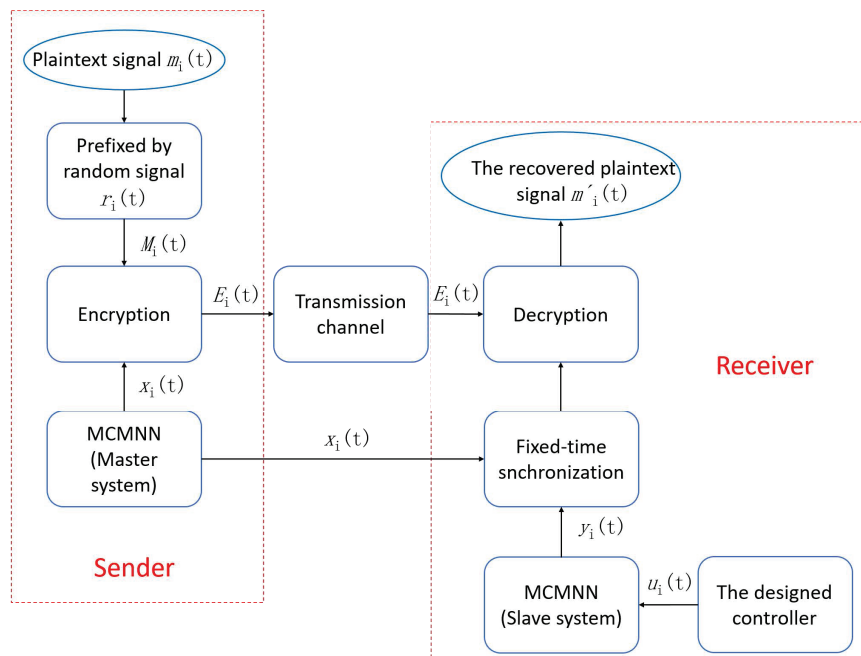


FIGURE 7 The schematic diagram of the proposed secure communication scheme.

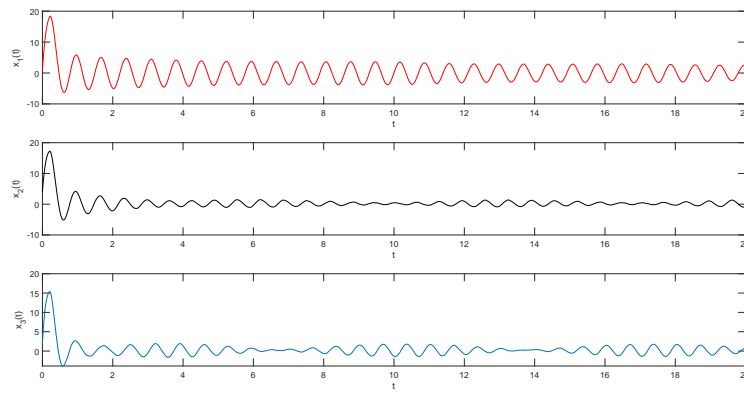


FIGURE 8 The state curve of single three-dimensional system (16).

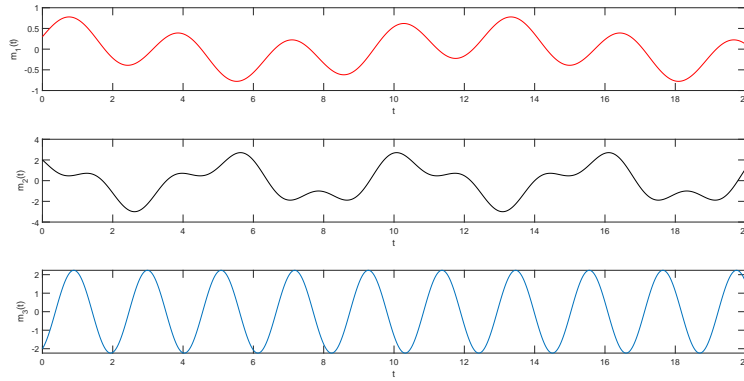


FIGURE 9 The time trajectory curve of plaintext signal.

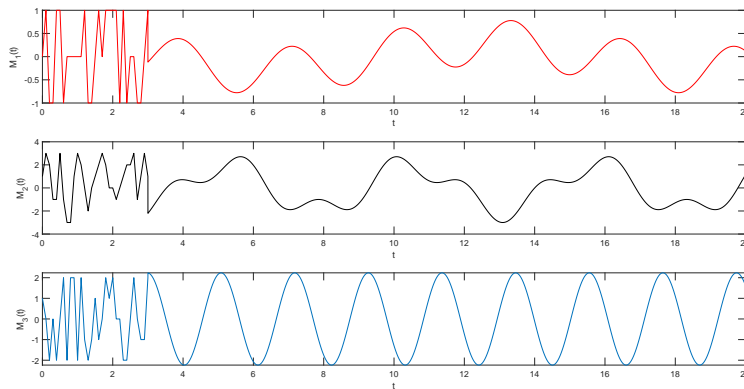


FIGURE 10 The time trajectory curve of mixed signal by plaintext signal and random signal.

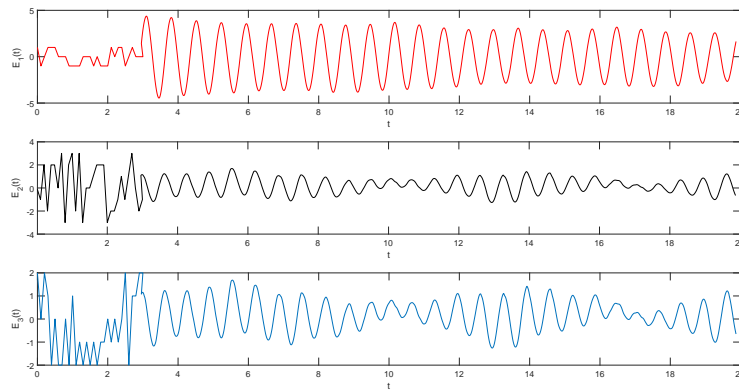


FIGURE 11 The time trajectory curve of encrypted signal.

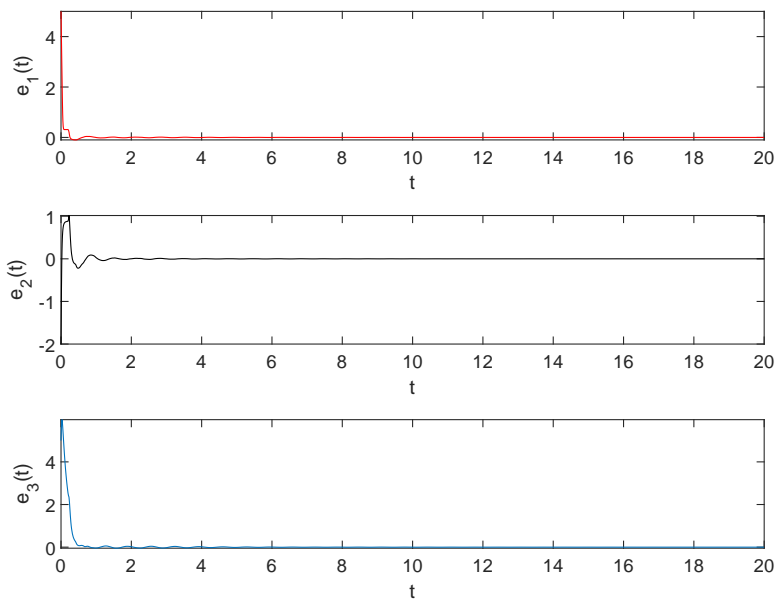


FIGURE 12 The error system of drive-response systems (17) and (18) with the controller.